ISSN: 2229-6956(ONLINE)
DOI: 10.21917/ijsc.2013.0083

DIAGNOSIS OF DIABETIC RETINOPATHY USING MACHINE LEARNING TECHNIQUES

R. Priya[1] and P. Aruna[2]
Department of Computer Science and Engineering, Annamalai University, India
E-mail: [1]prykndn@yahoo.com and [2]arunapuvi@yahoo.co.in

Abstract
Diabetic retinopathy (DR) is an eye disease caused by the complication of diabetes and we should detect it early for effective treatment. As diabetes progresses, the vision of a patient may start to deteriorate and lead to diabetic retinopathy. As a result, two groups were identified, namely non-proliferative diabetic retinopathy (NPDR) and proliferative diabetic retinopathy (PDR). In this paper, to diagnose diabetic retinopathy, three models like Probabilistic Neural network (PNN), Bayesian Classification and Support vector machine (SVM) are described and their performances are compared. The amount of the disease spread in the retina can be identified by extracting the features of the retina. The features like blood vessels, haemmoraghes of NPDR image and exudates of PDR image are extracted from the raw images using the image processing techniques and fed to the classifier for classification. A total of 350 fundus images were used, out of which 100 were used for training and 250 images were used for testing. Experimental results show that PNN has an accuracy of 89.6 % Bayes Classifier has an accuracy of 94.4% and SVM has an accuracy of 97.6%. This infers that the SVM model outperforms all other models. Also our system is also run on 130 images available from "DIARETDB0: Evaluation Database and Methodology for Diabetic Retinopathy" and the results show that PNN has an accuracy of 87.69% Bayes Classifier has an accuracy of 90.76% and SVM has an accuracy of 95.38%.

Keywords:
Probabilistic Neural Network, Bayesian Classification, Support Vector Machine, Sensitivity, Specificity, Accuracy

1. INTRODUCTION

Diabetes is a group of metabolic diseases in which a person has high blood sugar, either because the body does not produce enough insulin, or because the cells do not respond to the insulin that is produced. [27] Diabetic retinopathy is one of the common complications of diabetes. It is a severe and widely spread eye disease. It damages the small blood vessels in the retina resulting in loss of vision. The risk of the disease increases with age and therefore, middle aged and older diabetics are prone to Diabetic Retinopathy. Non-proliferative diabetic retinopathy is an early stage of diabetic retinopathy. In this stage, tiny blood vessels within the retina leak blood or fluid. The leaking fluid causes the retina to swell or to form deposits called exudates. Proliferative diabetic retinopathy, PDR is an attempt by the eye to grow or re-supply the retina with new blood vessels (neovascularization), due to widespread closure of the retinal blood supply. [28] Unfortunately, the new, abnormal blood vessels do not re-supply the retina with normal blood flow, but bleed easily and are often accompanied by scar tissue that may wrinkle or detach the retina.

In this paper, an automated approach for classification of the disease diabetic retinopathy using fundus images is presented. We used the retinal fundus images collected at the "Aravind Eye Hospital and Postgradute Institute of Opthalmology", Cuddalore Road Thavalakuppam Junction, Pondicherry. The retinal image is taken in the RGB form by fundus camera. A fundus camera or retinal camera is a specialized low power microscope with an attached camera designed to photograph the interior surface of the eye, including the retina, optic disc, macula, and posterior pole. [29] The images were captured using a Canon TopCon TRC-50 EX with Nicon retinal camera at a field-of-view (FOV) of 50°. The acquired image resolution is 1280 ×1024 in 24bit JPEG format. The evaluation of the proposed automated diagnosis system of diabetic retinopathy has been performed by using a set of 250 fundus images which is a combination of normal, NPDR and PDR affected images. The original image is converted to gray scale image. After that, adaptive histogram equalization is applied to improve the contrast of the image. Then, Discrete Wavelet Transform (DWT) is applied and the size of the image is reduced into half as 640 × 512 [30]. Then Matched filter response (MFR) is applied to reduce the noise in the image.

Finally, Fuzzy C-means clustering is applied to segment the blood vessels in the image. After preprocessing of images is completed, features such as Radius, Diameter, Area, Arc length, Centre Angle and Half area are calculated for each image. Then Modeling Techniques like PNN, Bayes Theory and SVM are used and their performances are compared. Finally, the images are classified into three groups namely, normal image, Non-Proliferative Diabetic Retinopathy (NPDR) and Proliferative Diabetic Retinopathy (PDR).

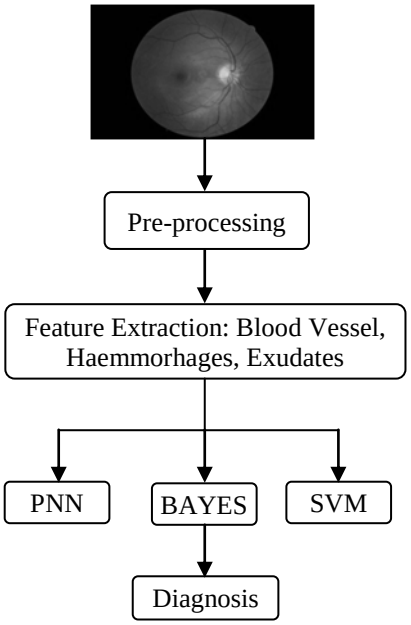

Fig.1. Block diagram for comparison between three classifiers for diagnosis of DR

The remainder of this paper is organized as follows. Section 2 describes the related work. Section 3 explains the preprocessing of images. Section 4 explains the feature extraction. Section 5 explains the feature values obtained. Section 6 describes the classification of DR disease using Support Vector Machine. Section 7 explains Probabilistic Neural Network and section 8 gives Bayesian Classification. Section 9 describes the results and discussion. Section 10 gives the conclusion. Fig.1 gives the block diagram for comparison of three classifiers for diagnosis of Diabetic Retinopathy.

2. RELATED WORK

During the recent years, there have been many studies on automatic diagnosis of diabetic retinopathy using several features and techniques. D. Vallabha et al. [1] proposed a method for automated detection and classification of vascular abnormalities in Diabetic Retinopathy using scale and orientation selective Gabor filter banks. R. Sivakumar et al. [2] presented a method to classify diabetic retinopathy subjects from changes in visual evoked potential spectral components. According to Thomas Walter et al. [3] exudates are found using their high grey level variation, and their contours are determined by means of morphological reconstruction techniques. HT Nguyenl et al. [4] proposed a multilayer feed forward network for the classification of DR. María García et al. [5] used a multilayer perceptron (MLP) classifier to obtain a final segmentation of Hard Exudates in the image. In [6], P. V. Nageswara rao et al. proposed a new approach for protein classification based on a Probabilistic Neural Network and feature selection. S. Chaudhury et al. [7] address the problem of detecting blood vessels in retinal images. They have used the concept of matched filter for detection of signals to detect piecewise linear segments of blood vessels in retinal images and constructed 12 different templates to search for vessel segments along all possible directions. In [8] Alireza Osareh et al. classified the segmented regions into two disjoint classes, exudates and non-exudates, comparing the performance of various classifiers. In [9] Wong Li Yun et al. Classified the four eye diseases using a three-layer feed forward neural network.

In [13], R. Priya and P. Aruna used SVM for the detection of diabetic retinopathy stages using color fundus images. In [14] Computer-assisted automated red lesion detection was performed on digitized transparencies. [15] This paper investigates and proposes a set of optimally adjusted morphological operators to be used for exudate detection on diabetic retinopathy patients non-dilated pupil and low-contrast images. [16] described a method for automatically detecting new vessels on the optic disc using retinal photography. The 'matched filter response' method is a widely used template-based technique that uses a set of 2D Gaussian kernels with a fixed length and orientation to enhance the vessels. In [17], a postprocessing technique, based on edge detection, is applied to distinguish hard exudates from cotton wool spots and other artefacts. In [18] Keith A. Goatman et al. described a method for automatically deducting new vessels on the optic disc using retinal photography. Aliaa Abdel-Haleim et al. [23] presented a method to automatically detect the position of the OD in digital retinal fundus images. The method starts by normalizing luminosity and contrast throughout the image using illumination equalization and adaptive histogram equalization methods respectively.

3. PREPROCESSING OF IMAGES

In detecting abnormalities associated with fundus image, the images have to be pre-processed in order to correct the uneven illumination, not sufficient contrast between exudates and image background pixels and the presence of noise in the input fundus image. The techniques for preprocessing include Gray scale Conversion, Adaptive Histogram Equalization, Discrete Wavelet Transform, Gaussian Matched Filter Response and Fuzzy C-means Clustering for segmentation of blood vessels.

3.1 GRAY SCALE CONVERSION

The acquired image resolution is 1280 × 1024 in 24bit JPEG format. The color image of an eye is taken as input image and is converted to a grayscale image as shown in Fig.2 and Fig.3 respectively.

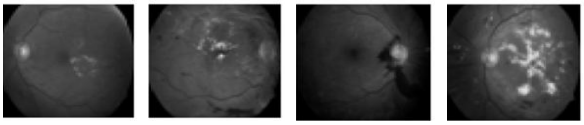

(a) (b) (c) (d)

Fig.2(a-d). Original DR affected Eye Image

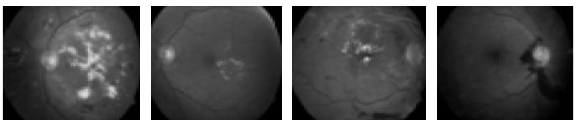

(a) (b) (c) (d)

Fig.3(a-d). Eye Image after Grey Scale Conversion

3.2 ADAPTIVE HISTOGRAM EQUALIZATION

Adaptive histogram equalization which is used to improve contrast in images is applied to the gray scale converted eye image. Consider a running sub image W of $N \times N$ pixels centered on a pixel $P(i, j)$, the image is filtered to produce another sub image P of ($N \times N$) pixels according to the equation below,

$$P_n = 255\left(\frac{[\phi_w(p) - \phi_w(Min)]}{[\phi_w(Max) - \phi_w(Min)]}\right) \quad (1)$$

where,
$$\phi_w(P) = \left[1 + \exp\left(\frac{\mu_w - p}{\sigma_w}\right)\right]^{-1} \quad (2)$$

and Max and Min are the maximum and minimum intensity values in the, whole eye image while μ_w indicate the local window mean and σ_w indicate standard deviation which are defined as,

$$\mu_w = \frac{1}{N^2} \sum_{(i,j)\varepsilon(k,l)} P(i, j) \quad (3)$$

$$\sigma_w = \sqrt{\frac{1}{N^2} \sum_{(i,j)\varepsilon(k,l)} (P(i, j) - \mu_w)^2} \quad (4)$$

As a result of this adaptive histogram equalization, the dark area in the input eye image that was badly illuminated has

become brighter in the output eye image while the side that was highly illuminated remains or reduces so that the whole illumination of the eye image is same as shown in Fig.4.

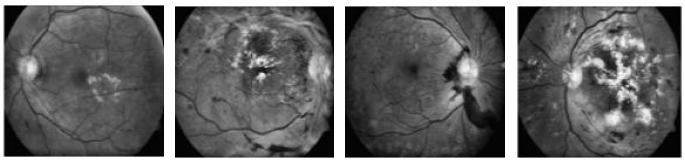

(a) (b) (c) (d)

Fig.4(a-d). Eye Images after Adaptive Histogram Equalization

3.3 DISCRETE WAVELET TRANSFORM

The transform of a signal is just another form of representing the signal. It does not change the information content present in the signal. The Discrete Wavelet Transform (DWT), which is based on sub-band coding, is found to yield a fast computation of Wavelet Transform. It is easy to implement and reduces the computation time and resources required. Wavelet transform decomposes a signal into a set of basis functions.

These basis functions are called wavelets. Wavelets are obtained from a single prototype wavelet $\psi(t)$ called mother wavelet by dilations and shifting,

$$\psi_{a,b}(t) = \frac{1}{\sqrt{a}}\psi(\frac{t-b}{a}) \quad (5)$$

where, 'a' is the scaling parameter and 'b' is the shifting parameter. The mother wavelet used to generate all the basis functions are designed based on some desired characteristics associated with that function. DWT2 is a Single-level discrete 2-D wavelet transform [35]. The dwt2 command performs a single - level two-dimensional wavelet decomposition with respect to either a particular wavelet or particular wavelet decomposition filters. [cA,cH,cV,cD] = dwt2 (X,'wname') computes the approximation coefficient matrix cA and details coefficients matrices cH, cV, and cD for horizontal, vertical, and diagonal, respectively, obtained by wavelet decomposition of the input matrix X where X is the given input eye image after applying adaptive histogram equalization. The 'wname' string contains the wavelet name. Haar wavelet is used. As a result of applying this DWT to the eye images, the size of the images is reduced to half without any change in the information content of an image. So the size of the eye images is now 640 × 512. The resulting images are shown in Fig.5.

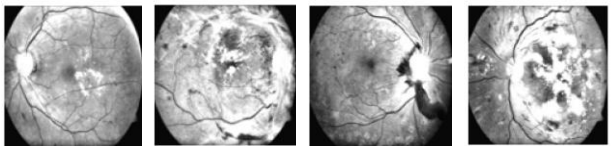

(a) (b) (c) (d)

Fig.5(a-d). Images after applying Discrete Wavelet Transform

3.4 THE MATCHED FILTER RESPONSE

The matched filter is the optimal linear filter for maximizing the signal to noise ratio (SNR) in the presence of additive stochastic noise. The optimal filter is given by,

$$h_{opt}(d) = -\exp(-d^2/2\sigma^2) \quad (6)$$

The negative sign indicates that the vessels are darker than the background. Also, instead of 'n' different types of objects having to be identified, the problem reduces to decide whether or not a particular pixel belongs to a blood vessel. If the magnitude of the filtered output at a given pixel location exceeds a certain threshold, the pixel is labeled as a part of a vessel. Instead of matching a single intensity profile of the cross section of a vessel, a significant improvement can be achieved by matching a number of cross sections (of identical profile) along its length simultaneously. Such a kernel may be mathematically expressed as,

$$K(x,y) = -\exp(-x^2/2\sigma^2) \quad (7)$$
$$\text{for } |y| \le L/2$$

where, L is the length of the vessel segment that has the same orientation, σ defines the spread of the intensity profile. Here we have taken L = 7 and σ = 2. The values are chosen heuristically. The intensity profile has a Gaussian shape. The square shape is used for the kernel. A maximum of twelve kernels was used to rotate by an amount of 15° to detect blood vessels. [24] To be able to detect vessels on all possible orientations, the kernel must be rotated to all possible vessel orientations and the maximum response from the filter bank is registered. As a result of applying this MFR to retinal images, response due to the noise is suppressed significantly, where no blood vessel is present as shown in Fig.6.

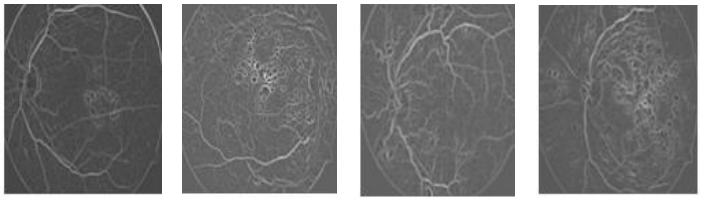

(a) (b) (c) (d)

Fig.6(a-d). Images after applying Matched Filter Response

3.5 THE FUZZY C-MEANS SEGMENTATION

Fuzzy C-means Segmentation (FCM) is a method of clustering which allows one piece of data to belong to two or more clusters. Here it is used to segment the input eye image and detect the blood vessels. Information about blood vessels can be used in grading disease severity or as part of the process of automated diagnosis of diseases with ocular manifestations. It is based on minimization of the following objective function,

$$J_m = \sum_{i=1}^{N}\sum_{j=1}^{C} u_{ij}^m \left\| x_i - c_j \right\|^2, \; 1 \le m < \alpha \quad (8)$$

where, m is the fuzzy co-efficient , any real number greater than 1, u_{ij} is the degree of membership of x_i in the cluster j, x_i is the i^{th} of d-dimensional measured data, c_j is the d-dimension center of the cluster, and ||*|| is any norm expressing the similarity between any measured data and the center. The algorithm is composed of the following steps [36],

Step 1: Initialize $U = [u_{ij}]$ matrix, $U(0)$

Step 2: At k-step: calculate the centers vectors $C(k) = [c_j]$ with $U(k)$

Step 3: At k-step: calculate the centers vectors $C(k) = [c_j]$ with $U(k)$

$$c_j = \frac{\sum_{i-1}^{N} u_{ij}^m \cdot x_i}{\sum_{i-1}^{N} u_{ij}^m}$$

Step 4: Update $U(k)$, $U(k + 1)$

$$u_{ij} = \frac{1}{\sum_{k-1}^{c} \left(\frac{\|x_i - c_j\|}{\|x_i - c_k\|} \right)^{\frac{2}{m-1}}}$$

Step 5: If $\| U(k + 1) – U(k)\| < \varepsilon$ then STOP; otherwise return to step 2.

Here we have taken $m = 2$ and $\varepsilon = 0.3$. The resulting images after applying Fuzzy C-means Segmentation is shown in Fig.7 below.

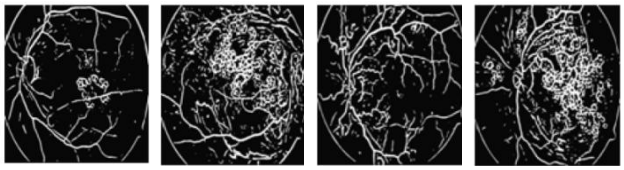

(a) (b) (c) (d)

Fig.7(a-d). Images after applying Fuzzy C-Means Clustering

4. FEATUREEXTRACTION [HAEMORAGHES, EXUDATES]

Both Hemorrhages and Exudates appear as bright lesions in retinopathies images and have sharp edges and high contrast with the back- ground. We perform boundary detection for exudates using thresholding and morphological processing algorithms. Fig. 8 gives the Block diagram for Haemorrhages or Exudates Detection. The following steps are applied to detect the Haemorrhages or Exudates.

4.1 GREEN COMPONENT

The retinal image is taken in the RGB form by fundus camera. The green channel of the RGB space is extracted and chosen for detection of exudates because exudates appear most contrasted in this channel. So the first step is to separate this channel to a new image

4.2 THRESHOLDING

Thresholding is a simple shape extraction technique, where the images could be viewed as the result of trying to separate the eye from the background. Thresholding is a method of producing regions of uniformity within an image based on some threshold criterion, *T*. The *T* can be defined as,

$$T = T\{x, y, A(x, y), f(x, y)\} \quad (9)$$

where, $f(x, y)$ is the gray level of the pixel at (x, y) and $A(x, y)$ denotes some local property in the neighborhood of this pixel.

A thresholded image,

$$g(x,y) = 1 \text{ if } f(x,y) \geq T \quad (10)$$

$$g(x,y) = 0 \text{ if } f(x,y) < T \quad (11)$$

A Local Thersholding technique is one that partitions the given image into sub-images and determines the threshold for each of these sub-images.

$$T = T\{A(x, y), f(x, y)\} \quad (12)$$

where, T is dependent upon a neighbourhood property of the pixel well as its grey-level value. The main task of thresholding is to highlight high values of wavelet coefficients which almost correspond to the optic disc and suppress small values which correspond to noise or unimportant structures in the image. To the morphologically eroded image, local thresholding is applied.

4.3 MORPHOLOGICAL PROCESSING

Erosion involves the removal (alteration) of pixels at the edges of regions, for example changing binary 1 value to 0, while dilation is the reverse process with regions growing out from their boundaries. These two processes are often carried out using a form of kernel known as a structural element. A structural element is an $N \times N$ kernel with entries classified according to a binary scheme, typically as 0 or 1. If all entries are coded 1 then the structural element is a solid square block, the center of which is laid over each pixel in the source image in turn.

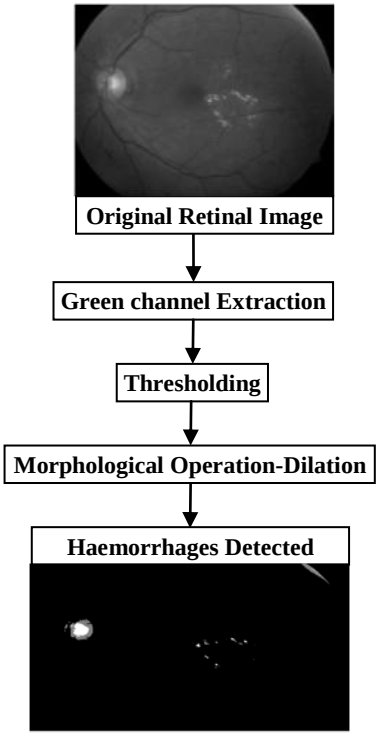

Fig.8. Block diagram for Haemorrhages Detection

The shape of the structural element may vary, for example as a vertical bar, horizontal bar, cross shape or a user-defined pattern. If dilation is followed by erosion the process is described as a Closing operation, whilst Erosion followed by dilation is known as Opening. These processes are not symmetric, and thus are generally not reversible. Opening eliminates small and thinner features, resulting in smoother edged regions, while closing also smoothes shapes but makes thin narrow features larger and eliminates small holes and narrow gaps. Here Dilation is used after thresholding and the

exudates or Haemorrhages are detected. Fig.9 gives the NPDR and PDR affected images and their corresponding Haemmorrages and Exudates detected images.

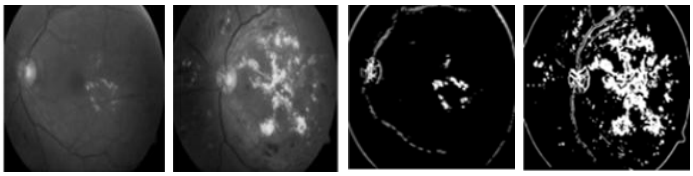

(a) (b) (c) (d)

Fig.9. (a). NPDR Image (b). PDR Image (c). Haemorrhages Detected Image (d). Exudates Detected Image

5. FEATURE VALUES

After performing the above mentioned preprocessing steps, the new eye image that is blood vessel detected image and Haemorrhages or exudates detected images are obtained. A set of feature values is taken from both blood vessel and Haemorrhages or exudates detected images. The feature values that are extracted are: Radius, Diameter, Area, Arc length, Center Angle and Half Area. Table.1 gives the range of feature values obtained for DR Diagnosis in our work. Fig.10 – Fig.12 gives the box plot graphs for the feature values obtained.

a. *Radius*

The radius of the circle is determined by using the formula, Radius

$$r = \frac{\sqrt{area}}{\pi} \tag{13}$$

π is approximately 3.142

b. *Diameter*

The diameter of the circle is determined by using the formula, Diameter

$$d = 2r \tag{14}$$

c. *Area*

$$\text{Area} = \pi r^2 \tag{15}$$

d. *Arclength*

The length of an arc is determined by using the formula

$$\text{Arclength} = R\left(\frac{2\pi C}{360}\right) \tag{16}$$

C is the center angle of the arc; R is the radius of the arc

e. *Center Angle*

A center angle is determined by using the formula,

$$\text{Center Angle} = \frac{Perimeter}{360}(2\pi r) \tag{17}$$

f. *Half Area*

Half area is determined by using the formula

$$\text{Half Area} = \frac{\text{Area of circle}}{2} \tag{18}$$

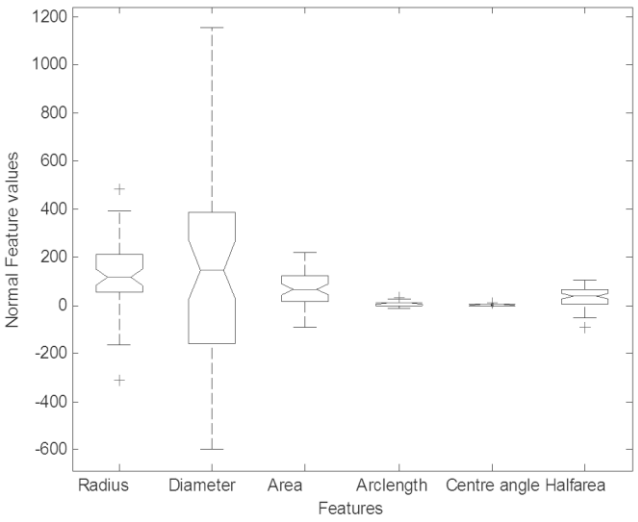

Fig.10. Box plot showing the feature values for Normal Images

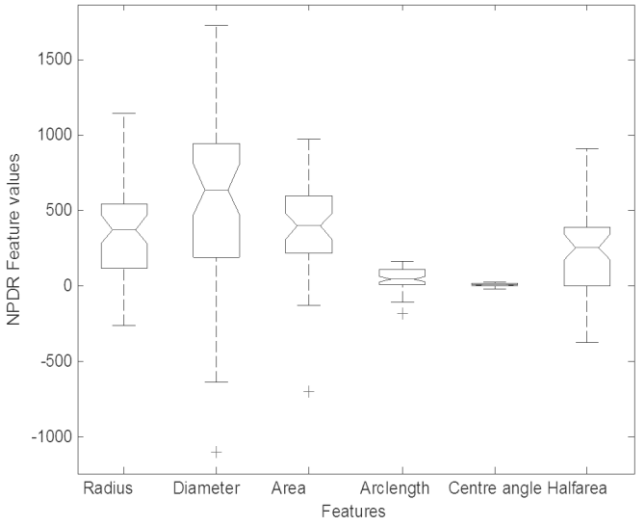

Fig.11. Box plot showing the feature values for NPDR Images

Table.1. The range of the feature values obtained for DR

Features / Types of Eye Images	Radius (cm)	Diameter (cm)	Area (cm^2)	Arc length (cm)	Centre angle (ϕ)	Half area (cm^2)
Normal	144-156	260 - 320	65 - 80	5.7 - 7.6	2.2 - 2.6	32 - 39
NPDR	311 - 346	625 - 643	304 - 324	60.9 - 63.6	10.6 - 11.3	249 - 254
PDR	421 - 426	843 - 854	558 - 572	143 - 148	19.4 - 19.8	279 - 284

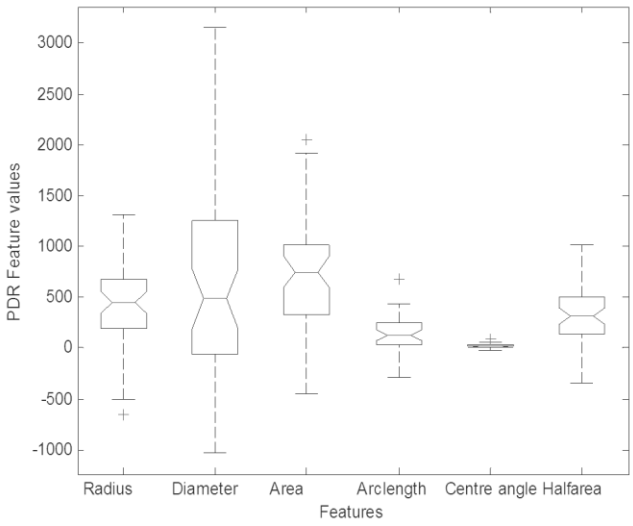

Fig.12. Box plot showing the feature values for PDR Images

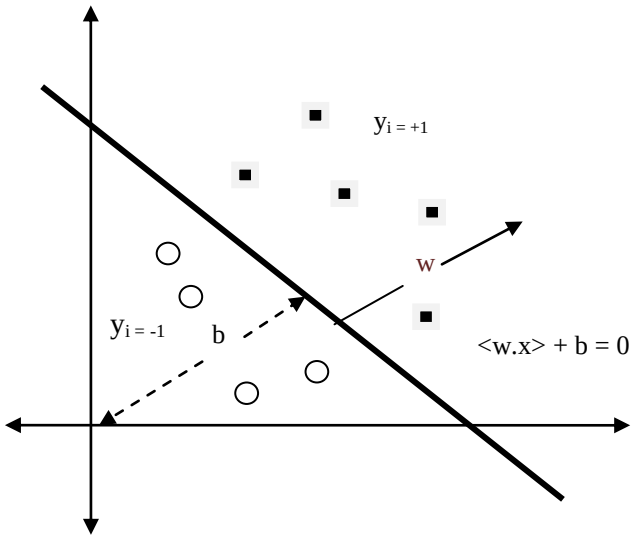

Fig.13. A separating hyperplane (w, b) for a two dimensional (2D) training set

6. SUPPORT VECTOR MACHINE

SVM is a robust technique for data classification and regression. It is described in detail by Vapnik [10]. In pattern recognition we are given training data in the form,

$$(x_1, y_1),\ldots..,(x_e, y_e) \in R^n \times \{+1, -1 \qquad (19)$$

that is *n*–dimensional patterns (vectors) x_i and their labels y_i. [32] A label with the value of +1 denotes that the vector is classified in class +1 and a label of −1 denotes that the vector is part of class −1. We thus try to find a function $f(x) = y$: $R^n \rightarrow \{+1, -1\}$ that apart from correctly classifying the patterns in the training data correctly classifies unseen patterns too. This is called generalization. SVMs are based on the class of hyperplanes

$$\langle w \cdot x \rangle + b = 0; w \in R^n, b \in R, \qquad (20)$$

which basically divide the input space into two: one part containing vectors of the class −1 and the other containing those that are part of class +1 as shown in Fig.13. If there exists such a hyperplane, the data is said to be linearly separable. To find the class of a particular vector *x*, we use the following decision function,

$$f(x) = sign(\langle w \cdot x \rangle + b) \qquad (21)$$

There may be more than one hyperplane that correctly classifies the training examples (for instance, in Fig.13 the hyperplane could be closer to class −1). It has been shown that the hyperplane that guarantees the best generalization performance is the one with the maximal margin of separation between the two classes. This type of hyperplane is known as the optimal or maximal margin hyperplane and is unique. The optimal hyperplane can be constructed by solving a convex (no local minima, therefore any solution is global) optimization problem that is minimizing a quadratic function under linear inequality constraints. The solution to this problem has an expansion in terms of a subset of the training examples that lie on the margin, called support vectors as shown in Fig.14.

Support vectors contain all the information needed about the classification problem, since even if all the other vectors are removed the solution will still be the same, the optimization problem (used to find the optimal hyperplane) and the decision function can be expressed in dual form which depends only on dot products between vectors. The dual representation of the decision function is

$$f(x) = sign\left(\sum_{i=1}^{l} y_i \alpha_i \langle x \cdot x_i + b \rangle \right) \qquad (22)$$

where, $\alpha_i \in R$ is a real-valued variable that can be viewed as a measure of how much informational value x_i has. Thus for vectors that do not lie on the margin (i.e. non support vectors) this value will be zero. The optimal hyperplane classifier uses only dot products between vectors in input space. In feature space this will translate to $\langle \phi(x) \cdot \phi(y) \rangle$. A kernel is a function $K(x, y)$ that given two vectors in input space, returns the dot product of their images in feature space as shown in Fig.15. Thus, $K(x, y) = \langle \phi(x) \cdot \phi(y) \rangle$.

To construct an optimal hyperplane, SVM employs an iterative training algorithm, which is used to minimize an error function. [33] SVM training involves the minimization of the error function,

$$\frac{1}{2} w^T w + C \sum_{i=1}^{N} \xi_i \qquad (23)$$

subject to the constraints

$$y_i \left(w^T \phi(x_i) + b \right) \geq 1 - \xi_i$$

and $$\xi_i \geq 0, i = 1,..., N \qquad (24)$$

where, *C* is the capacity constant, *w* is the vector of coefficients, *b* a constant and ξ_i are parameters for handling nonseparable data (inputs). The index *i* labels the *N* training cases. $y \in \pm 1$ is the class labels and x_i is the independent variables. The kernel ϕ is used to transform data from the input (independent) to the feature space. SVM Torch is used in our work. We have used polynomial kernel which is given by,

$$K(x, x') = (x.x' + 1)^d \quad (25)$$

where, x and x' are the feature vectors for the three classes, d is the kernel parameter. Support vector machine training process is applied to analyze training data to find an optimal way to classify images into their respective classes. The size of the input training vector is 250 * 6. The output can be one of the three classes namely normal, NPDR and PDR.

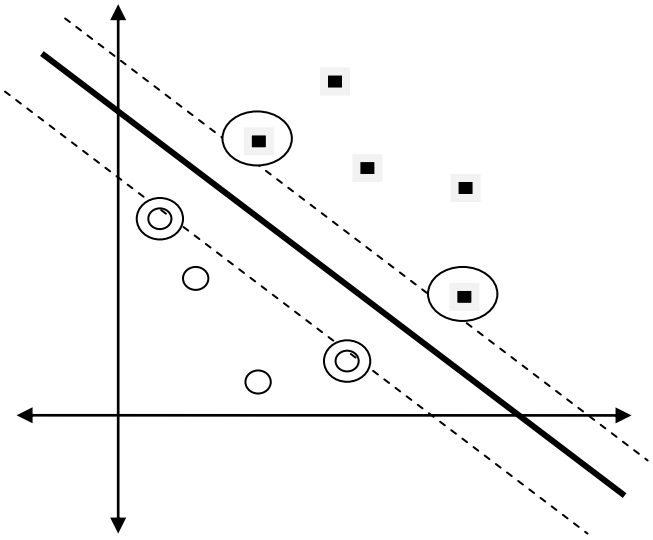

Fig.14. A maximal margin hyperplane with its support vectors encircled

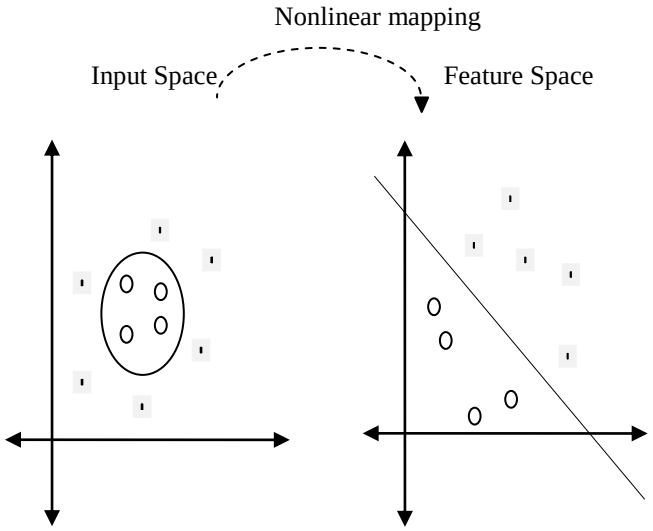

Fig.15. A nonlinear mapping from the input space to feature space can simplify the classification task

7. PROBABILISTIC NEURAL NETWORK

The PNN was first proposed in [11]. The PNN architecture is composed of many interconnected processing units or neurons organized in successive layers. [12] The input layer unit does not perform any computation and simply distributes the input to the neurons in the pattern layer. On receiving a pattern x from the input layer x, the neuron of the pattern layer computes its output

$$\phi_{ij}(x) = \frac{1}{(2\pi)^{\frac{d}{2}}\sigma^d} \exp[-\frac{(x - x_{ij})^T (x - x_{ij})}{2\sigma^2}] \quad (26)$$

where, d denotes the dimension of the pattern vector x, σ is the smoothing parameter and x_{ij} is the neuron vector. The summation layer neurons compute the maximum likelihood of pattern x being classified into c_i by summarizing and averaging the output of all neurons that belong to the same class

$$P_i(x) = \frac{1}{(2\pi)^{\frac{d}{2}}\sigma^d} \frac{1}{N_i} \sum_{j=1}^{N_i} \exp\left[-\frac{(x - x_{ij})^T (x - x_{ij})}{2\sigma^2}\right] \quad (27)$$

where, N_i denotes the total number of samples in class C_i. If the apriori probabilities for each class are the same, and the losses associated with making an incorrect decision for each class are the same, the decision layer unit classifies the pattern in accordance with the Bayes's decision rule based on the output of all the summation layer neurons

$$\hat{C}(x) = \arg\max\{P_i(x)\}, \quad i = 1,2,\ldots\ldots n \quad (28)$$

where, $\hat{C}(x)$ denotes the estimated class of the pattern x and m is the total number of classes in the training samples. Fig.16 shows a configuration of the PNN with four layers. There were six input features, which created a six dimensional input vector (X_1, X_2, X_3, . . . , X_6). Each image had a combination of specific values of the input vector—called an input pattern—that described the operating features of the image. The PNN model classifies that image from its input pattern into one of three categories (Normal, NPDR, PDR) as follows: In the input layer, the number of neurons is equal to the number of input features. In the pattern layer, the total number of neurons is the sum of the number of neurons used to represent the patterns for each category.

Each category may contain many training patterns (training vectors) whose dimension is equal to the number of input factors, and taking a set of specific values of input factors. The training vectors are imported from sample data and hence they are not always necessarily representative of all existing patterns for that class. However, this is the advantage of PNN, in that it can generalize to allow recognition of a new pattern of a class. The activation function used in the pattern layer, is the Gaussian kernel. In the summation layer, the number of neurons is equal to the number of categories. The activation is simply a weighted sum function. The outgoing signals can be adjusted according to loss and prior probability value. In the output layer, there is one neuron to represent the classification result. The activation function is an arg max function, which outputs the category associated with the largest value between incoming signals. Suppose, Wdn is the input to the pattern layer for '*d*' varies from 1, 2,... 250, corresponding to 250 tested images and 'n' varies from 1, 2,....., 6 corresponding to the feature vector. The pattern layer can be processed and the output layer has a node for each pattern classification. The sum for each hidden node is sent to the output layer and the highest value wins. This method has been done for three classes namely normal, NPDR and PDR.

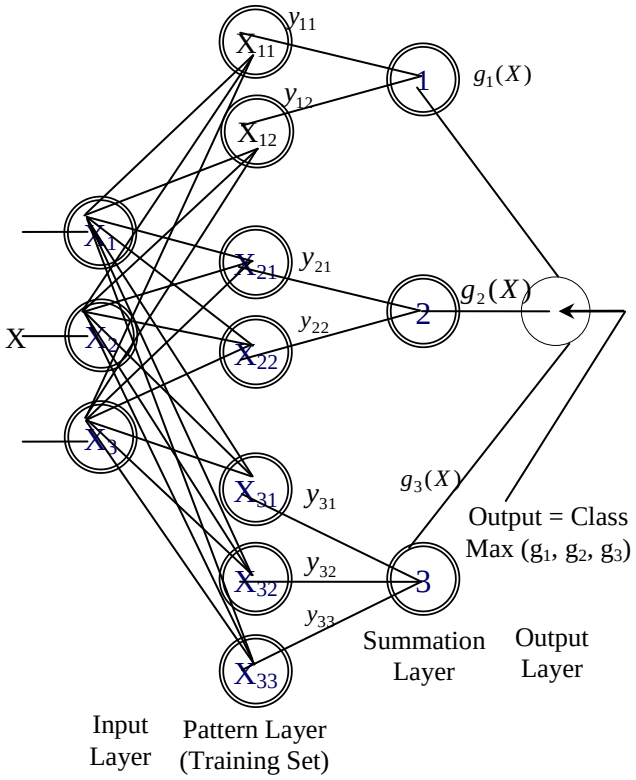

Fig.16. Architecture of Probabilistic Neural Network

8. BAYESIAN CLASSIFICATION

The Bayes classifier is a traditional statistic-based classifier that analyzes discriminant functions. A classifier assigns an input vector x to class C_k if $y_k(x) > y_j(x)$ for all $j \neq k$. By choosing $y_k(x) = PC_k/X$, this posterior probability is the probability of a pattern belonging to class C_k when we observe the input vector x. Bayes theory provides a method to calculate the probability of a hypothesis based on its prior probability, the probabilities of observing various data for the given hypothesis, and the observed data itself. We can detect the Diabetic Retinopathy affected image by using Bayes theory. It says that,

$$P(w_j|x) = \frac{P(x|w_j)P(w_j)}{P(x)} \quad (29)$$

a. x is the feature value of dimensions [250 * 6] of eye images.

b. $P(w_j/x)$ is the probability of disease like NPDR, PDR and normal for the given features like Radius, Diameter, Area, Arclength, Center Angle and Half Area.

c. $P(x)$ is the probability of feature values.

9. RESULTS AND DISCUSSION

The Proposed method was implemented in Matlab and Microsoft Visual Basic 6.0. The results of the classification Procedures are shown in Table.2. Table.3 shows the result of Sensitivity, Specificity and Percentage of accuracy for the three classes of eye images using the three classifiers. The ROC graphs are a useful technique for organizing classifiers and visualizing their performance. Fig.17 gives the comparison of ROC curve for the three models.

Table.2. Results of PNN, BAYES and SVM classification

Models	True Positive	True Negative	False Positive	False Negative
PNN	180	44	6	20
Bayes	190	46	4	10
SVM	196	48	2	4

Table.3. Results of sensitivity, specificity, % of accuracy

Models	Sensitivity	Specificity	Accuracy
PNN	90	88	89.6
Bayes	95	92	94.4
SVM	98	96	97.6

The quality assessment[QA] for fundus images was defined as "the characteristics of an image that allow the retinopathy diagnosis by a human or software expert" [34]. The performance of our implementation of the QA is evaluated with a standard benchmarking technique. The complete QA system is run on 130 images available from "DIARETDB0: Evaluation Database and Methodology for Diabetic Retinopathy". [31] Thus by utilizing the proposed database, it is now possible to compare our algorithms, and correspondingly, analyze their maturity for technology transfer from the research laboratories to the medical practice.

The size of the images in this database is 1500 × 1152. For the DIARETDB0 database the results of the classification Procedures are shown in Table.4 and Table.5 shows the result of Sensitivity, Specificity and Percentage of accuracy using the three classifiers.

Table.4. DIARETDB0 Database and the results obtained

	DIARET DB0	PNN	SVM	BAYES
Total number of images available and used for testing	130	130	130	130
Normal	20	14	18	16
Showing Signs of DR	110	100	106	102

Table.5. DIARETDB0 Database and results obtained

Models	True Positive	True Negative	False Positive	False Negative	Sensitivity	Specificity	Accuracy
PNN	100	14	6	10	90.90	70.00	87.69
Bayes	102	16	4	8	92.72	80.00	90.76
SVM	106	18	2	4	96.36	90.00	95.38

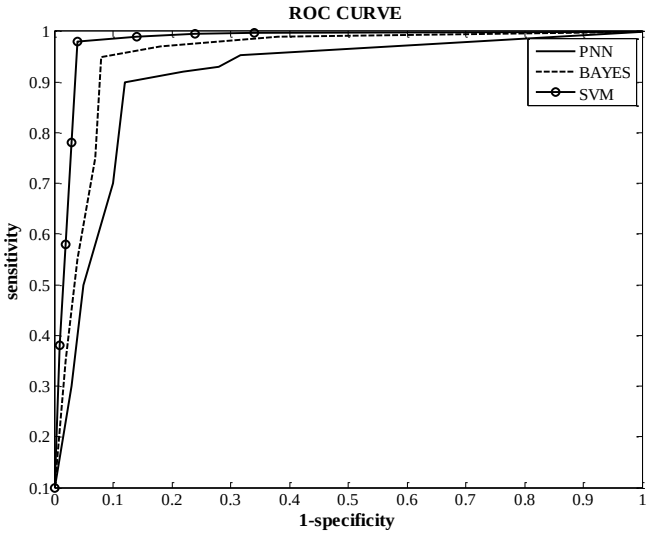

Fig.17. ROC Curve for Comparison of PNN, Bayes and SVM

Clearly, the three classification systems produce encouraging results. Sinthanayothin et al. [19] have differentiated diabetic retinopathy from normal retina using image processing algorithms. Their system, based on a multilayer perceptron neural network, yielded a sensitivity of 80.21% and a specificity of local, contrast enhancement. 70.66%. María García et al. [20] proposed to automatically detect one of these lesions, hard exudates (EXs), in order to help ophthalmologists in the diagnosis and follow-up of the disease. Using a lesion-based criterion, they achieved a mean sensitivity (SE) of 88.14% and a mean positive predictive value (PPV) of 80.72% for MLP. With RBF they obtained SE = 88.49% and PPV = 77.41%, while they reached SE = 87.61% and PPV = 83.51% using SVM. With an image-based criterion, a mean sensitivity (SEi) of 100%, a mean specificity (SP) of 92.59% and a mean accuracy (AC) of 97.01% were obtained with MLP. Using RBF they achieved SE = 100%, SP = 81.48% and AC = 92.54%. With SVM the image-based results were SE = 100%, SP = 77.78% and AC = 91.04%. Larsen et al. have used image processing algorithm for the detection of hemorrhages and microaneurysms to diagnose diabetic retinopathy [21].

Their algorithm demonstrated a specificity of 71.4% and a resulting sensitivity of 96.7% in detecting diabetic retinopathy when applied at a tentative threshold setting for use in diabetic retinopathy screening. A Osareh et al. [22] proposed to segment the colour retinal images using Fuzzy C-means clustering following some key preprocessing steps. To classify the segmented regions into exudates and non-exudates, an artificial neural network classifier was investigated. The proposed system achieved a diagnostic accuracy with 95.0% sensitivity and 88.9% specificity for the identification of images containing any evidence of retinopathy. In [25], Alireza Osareh, et al. present and compare two methods namely Neural Network based approach and the Support Vector Machine based approach for their classification and for identification of the Exudates pathologies in colour retinal images. In [26] Ahmad Fadzil M Hani et al. investigated the suitability of the Gaussian Bayes classifier in determining DR severity level.

Our system is far better as compared to the other works discussed so far. In our present work, we are able to identify normal, NPDR and PDR cases of the DR correctly with an accuracy of more than 80% and a sensitivity of more than 90% in all the three models. Among the three SVM outperforms all other models. Fig.18 – Fig.33 are the screenshots for diagnosing the retinal images as normal, Non-proliferative diabetic retinopathy or Pro-liferative retinopathy using PNN, Bayes and SVM Classification. In PNN, Image085 of DIARETDB0 Database as shown in Fig.19, was shown and diagnosed as Normal. Similarly, in SVM, Image 040 of DIARETDB0 as shown in Fig.24, was shown and diagnosed as PDR, Also, in BAYES, Image 018 of DIARETDB0 as shown in Fig.30, was shown and diagnosed as NPDR.

SCREENSHOTS FOR PNN CLASSIFICATION

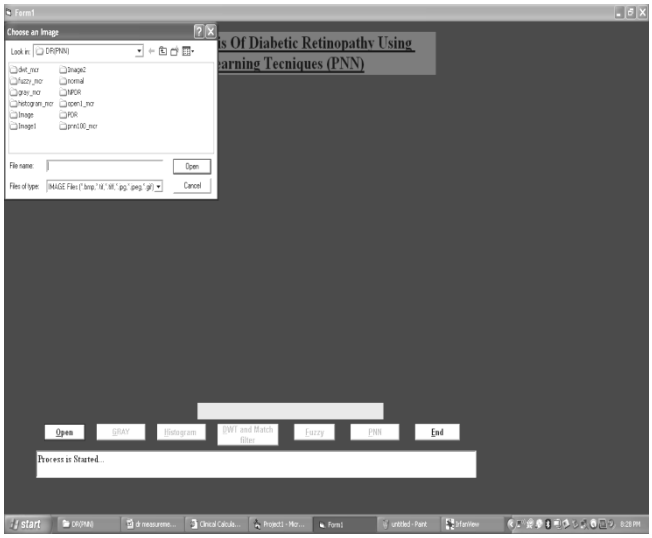

Fig.18. Snapshot for selecting an eye image

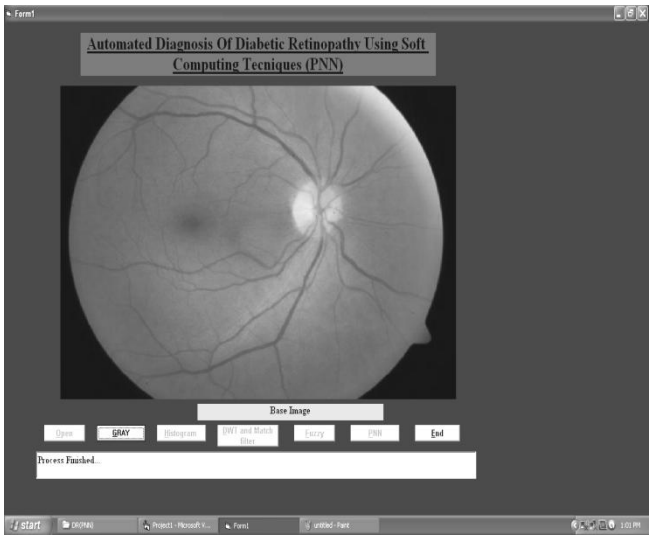

Fig.19. Snapshot of a loaded colour eye image[Image 085 of DIARETDB0: database]

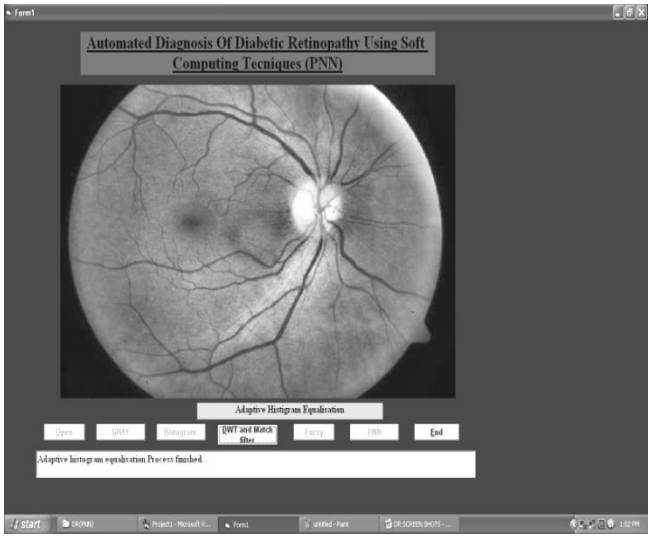

Fig.20. Snapshot of an eye image after Histogram Equalisation

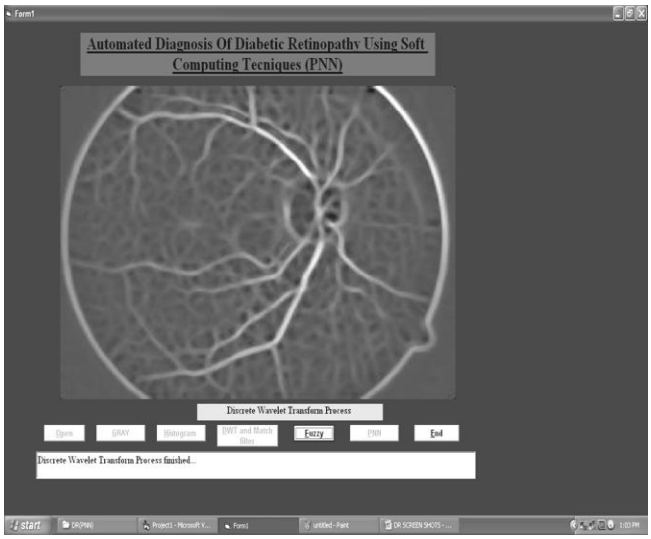

Fig.21. Snapshot of an eye image after Matched Filters

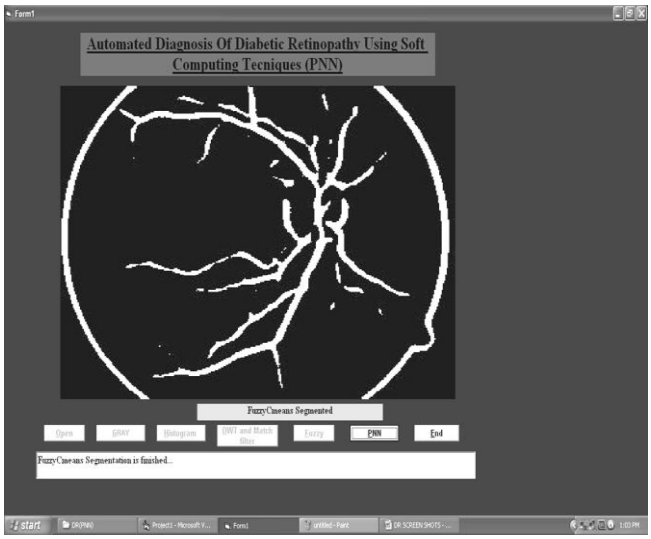

Fig.22. Snapshot of an eye image after Fuzzy C-means Segmentation

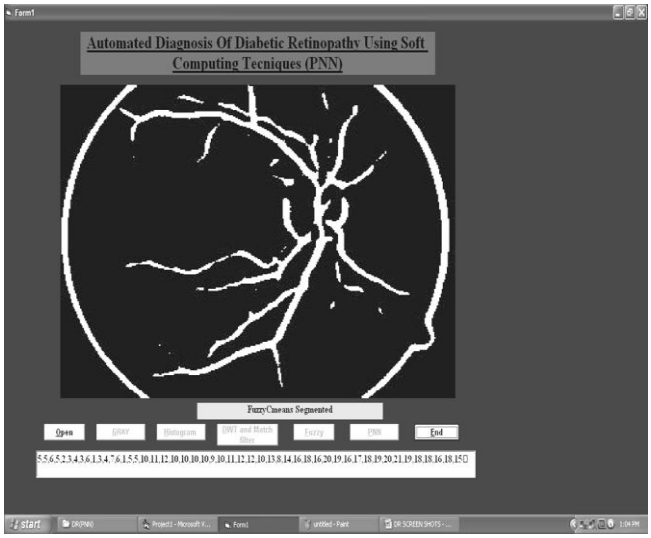

Fig.23. Snapshot showing the Process of PNN Results

SCREENSHOTS FOR SVM CLASSIFICATION

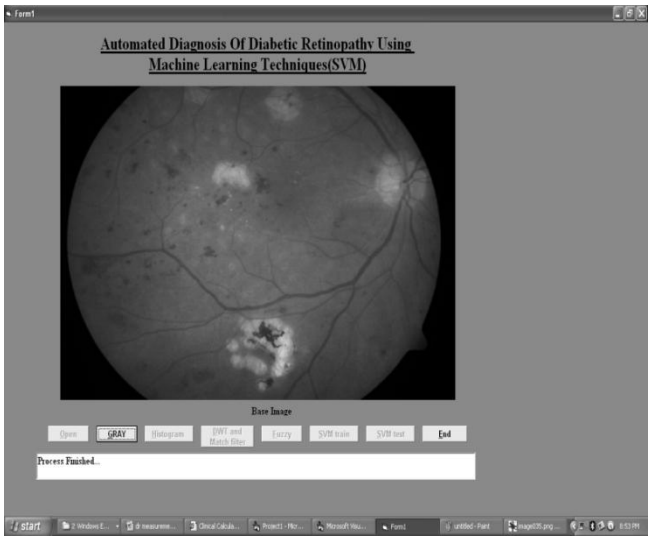

Fig.24. Snapshot of a loaded colour eye image [Image 040 of DIARETDB0: database]

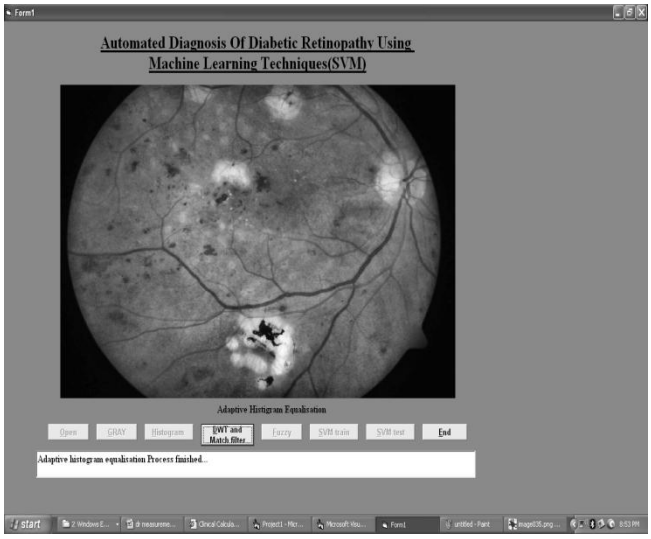

Fig.25. Snapshot of an eye image after Histogram Equalisations

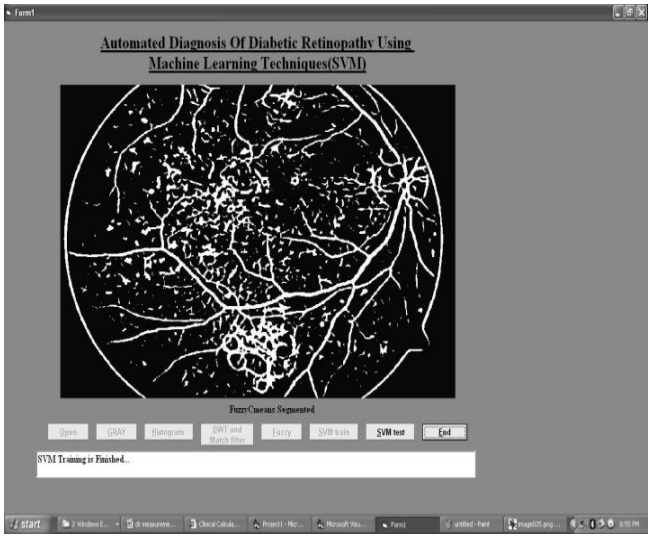

Fig.26. Snapshot of an eye image after Matched Filter

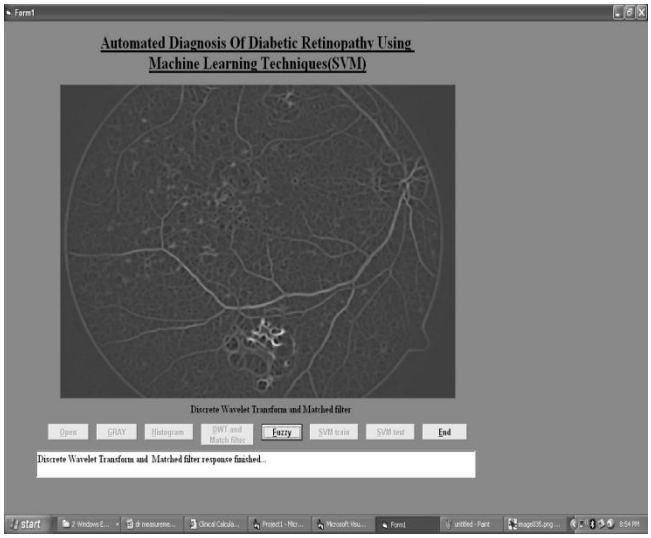

Fig.27. Snapshot showing the Process of SVM Training Equalisation

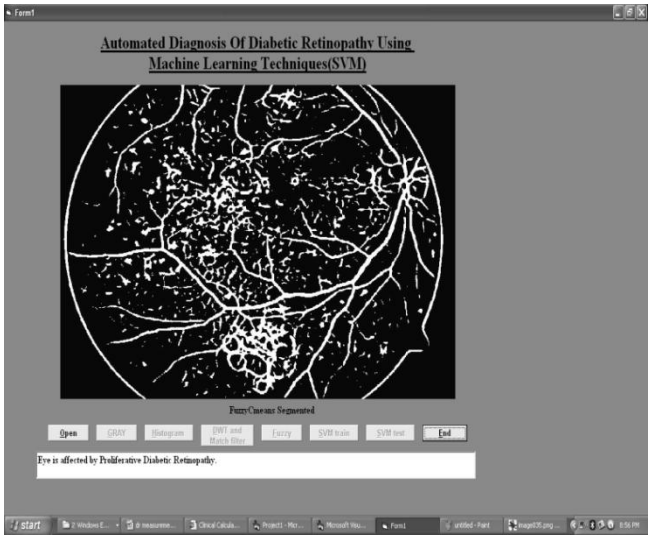

Fig.28. Snapshot for diagnosing the eye image as PDR after SVM testing

SCREENSHOTS FOR BAYES CLASSIFICATION

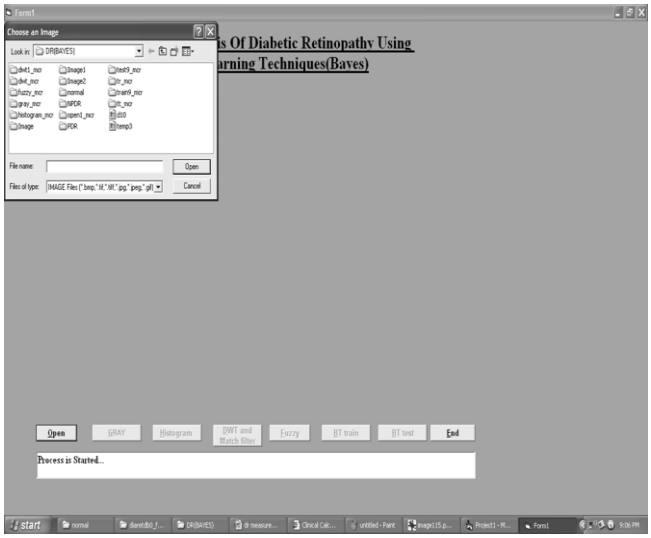

Fig.29. Snapshot for selecting an eye image

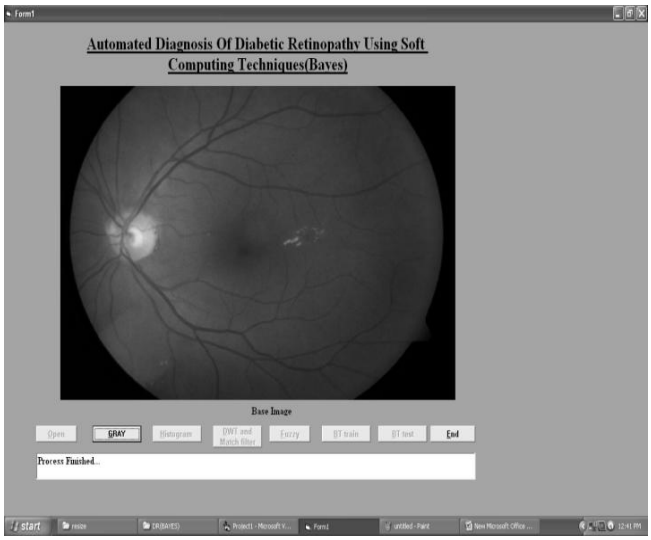

Fig.30. Snapshot of a loaded colour eye image Image 018 of DIARETDB0: database

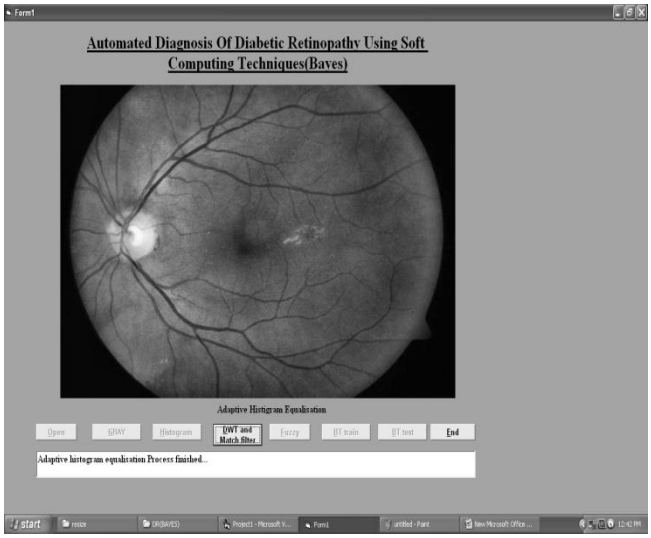

Fig.31. Snapshot of an eye image after Histogram Equalisation

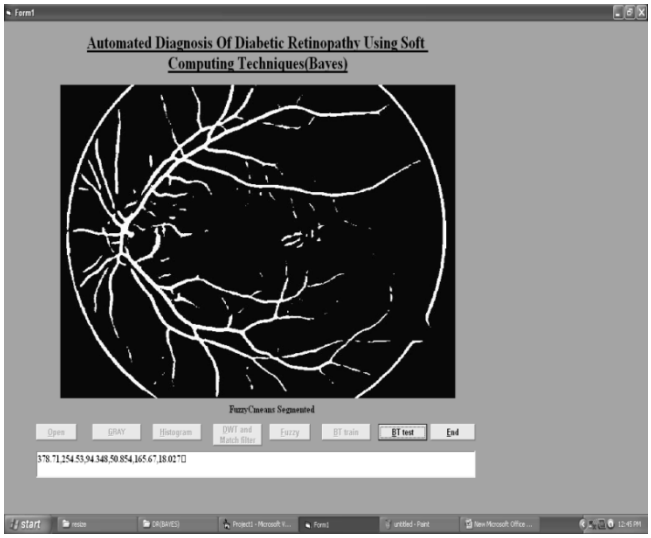

Fig.32. Snapshot showing the Process of Bayes Training

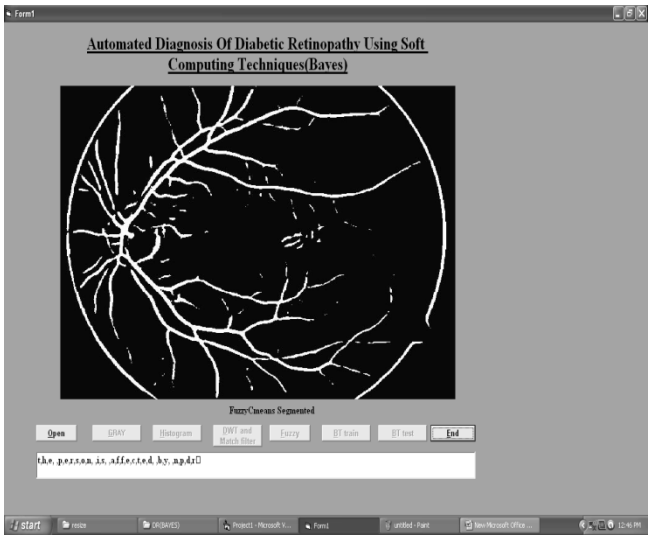

Fig.33. Snapshot for diagnosing the eye image as NPDR after Bayes Testing

10. CONCLUSION

Diabetic Retinopathy is a disease which causes vision loss rapidly. To the input color retinal images, preprocessing techniques like Grayscale conversion, Adaptive Histogram Equalization, Discrete Wavelet Transform, Matched filter Response and Fuzzy C-means segmentation are applied. After applying these pre-processing techniques the quality of the images are improved. From the pre-processed images, features were extracted for the classification process. As an achievement of this work, the DR has been classified into two categories NPDR and PDR using PNN, Bayes theory and SVM. All the three techniques used for the classification were good in performance, but SVM is more efficient than PNN and Bayes Theory from the obtained results. Thus this work has given a successful Diabetic Retinopathy Diagnosing method which helps to diagnose the disease in early stage which mutually reduces the manual work. Experimental results show that PNN has an accuracy of 89.6 % Bayes Classifier has an accuracy of 94.4% and SVM has an accuracy of 97.6%.

This infers that the SVM model outperforms all other models. Also our system is run on 130 images available from "DIARETDB0: Evaluation Database and Methodology for Diabetic Retinopathy" and the results show that PNN has an accuracy of 87.69% Bayes Classifier has an accuracy of 90.76% and SVM has an accuracy of 95.38%. However, we can improve the efficiency of the correct classification by extracting better features and by increasing the number of data in each class and also by combining with other pattern classification models.

REFERENCES

[1] D. Vallabha, R. Dorairaj, K. R. Namuduri and H. Thompson, "Automated Detection and Classification of Vascular Abnormalities in Diabetic Retinopathy", *38th Asilomar Conference on Signals, Systems and Computers*, Vol. 2, pp. 1625 – 1629, 2004.

[2] R. Sivakumar, G. Ravindran, M. Muthayya, S. Lakshminarayanan and C. U. Velmurughendran, "Diabetic Retinopathy Classification", *IEEE International Conference on Convergent Technologies for the Asia-Pacific Region*, Vol. 1, pp. 205 - 208, 2003.

[3] T. Walter, J. C. Klein, P. Massin and A. Erginay, "A contribution of image processing to the diagnosis of diabetic retinopathy-detection of exudates in color fundus images of the human retina", *IEEE Transactions on Medical. Imaging*", Vol. 21, No. 10, pp. 1236 – 1243, 2002.

[4] H. T. Nguyen, M. Butler, A. Roychoudhry, A. G. Shannon, J. Flack and P. Mitchell, "Classification of diabetic retinopathy using neural networks", *18th Annual International Conference of the IEEE Engineering in Medicine and Biology Society*, Vol. 4, pp. 1548 – 1549, 1996.

[5] María García, Roberto Hornero, Clara I. Sanchez, María I. Lopez and Ana Díez, "Feature Extraction and Selection for the Automatic Detection of Hard Exudates in Retinal Images", *Proceedings of the 29th Annual International Conference of the IEEE Engineering in Medicine and Biology Society Cite Internationale*, pp. 4969 – 4972, 2007.

[6] P. V. Nageswara Rao, T. Uma Devi, D. S. V. G. K. Kaladhar, G. R. Sridhar, Allam Appa Rao, "A Probabilistic Neural Network Approach for protein Superfamily Classification", *Journal of Theoretical and Applied Information Technology*, Vol. 6, No. 1, pp. 101, 2009.

[7] S. Chaudhuri, S. Chatterjee, N. Katz, M. Nelson and M. Goldbaim, "Detection of blood vessels in retinal images using two-dimensional matched filters", *IEEE Transactions on Medical Imaging*, Vol. 8, No. 3, pp. 263 – 269,1989.

[8] Alireza Osareh, Majid Mirmehdi, Barry Thomas and Richard Markham, "Classification and Localisation of Diabetic-Related Eye Disease", *Proceedings of the 7th European Conference on Computer Vision*, pp. 502 – 516, 2002.

[9] Wong Li Yun, U. Rajendra Acharya, Y. V. Venkatesh, Caroline Cheec, Lim Choo Min and E. Y. K. Ng "Identification of different stages of diabetic retinopathy

using retinal optical images", *Information Sciences*, Vol. 178, No. 1, pp. 106 – 121, 2008.

[10] V. N. Vapnik, "*Statistical Learning Theory*", New York: Wiley, 1998.

[11] D. F. Specht, "Probabilistic neural networks", *Neural Networks*, Vol. 3, No. 1, pp. 109 – 118, 1990.

[12] K. Z. Mao, K. C. Tan and W. Ser, "Probabilistic Neural-Network Structure Determination for Pattern Classification", *IEEE Transactions on Neural Networks*, Vol. 11, No. 4, pp. 1009 – 1016, 2000.

[13] R. Priya and P. Aruna, "Automated Classification System for Early Detection of Diabetic Retinopathy in Fundus Images", *International Journal of Applied Engineering Research*, Vol. 1, No. 3, 2010.

[14] Nicolai Larsen, Jannik Godt, Michael Grunkin, Henrik Lund-Andersen and Michael Larsen, "Automated Detection of Diabetic Retinopathy in a Fundus Photographic Screening Population", *Investigative Ophthalmology and Visual Science*, Vol. 44, No. 2, pp. 767 – 771, 2003.

[15] Akara Sopharak, Bunyarit Uyyanonvara, Sarah Barman and Thomas H. Williamson, "Automatic detection of diabetic retinopathy exudates from non-dilatedretinal images using mathematical morphology methods", *Computerized Medical Imaging and Graphics*, Vol. 32, No. 8, pp. 720 –727, 2008.

[16] A. Hoover, V. Kouznetsova and M. Goldbaum, "Locating blood vessels in retinal images by piecewise threshold probing of a matched filter response", *IEEE Transactions on Medical Imaging*, Vol. 19, No. 3, pp. 203 – 210, 2000.

[17] C. I. Sánchez, M. García, A. Mayo, M. I. López and R. Hornero, "Retinal image analysis based on mixture models to detect hard exudates", *Medical Image Analysis*, Vol. 13, No. 4, pp. 650 – 658, 2009

[18] Keith A. Goatman, Alan D. Fleming, Sam Philip, Graeme J. Williams, John A. Olson and Peter F. Sharp, "Detection of New Vessels on the Optic Disc Using Retinal Photographs", *IEEE Transactions on Medical Imaging*, Vol. 30, No. 4, pp. 972 – 979, 2011.

[19] C. Sinthanayothin, V. Kongbunkiat, S. Phoojaruenchanachai and A. Singalavanija, "Automated screening system for diabetic retinopathy", *Proceedings of the 3rd International Symposium on Image and Signal Processing and Analysis*, Vol. 2, pp. 951 – 920, 2003.

[20] Maria Garcia, Clara I. Sanchez, María I. Lopez, Daniel Abasolo and Roberto Hornero, "Neural network based detection of hard exudates in retinal images", *Computer Methods and Programs in Biomedicine*, Vol. 93, No. 1, pp. 9 – 19, 2009.

[21] M. Larsen, J. Godt, N. Larsen, H. Lund-Andersen, A. K. Sjolie, E. Agardh, H. Kalm, M. Grunkin and D. R. Owens, "Automated detection of fundus photographic red lesions in diabetic retinopathy", *Investigative Ophthalmology and Visual Science* ,Vol. 44, No. 2, pp. 761– 766, 2003.

[22] A. Osareh, M. Mirmehdi, B. Thomas and R. Markham, "Automated identification of diabetic retinal exudates in digital colour images", *British Journal of Ophthalmol*, Vol. 87, pp. 1220 – 1223, 2003.

[23] Aliaa Abdel-Haleim, Abdel-Razik Youssif, Atef Zaki Ghalwash, Amr Ahmed Sabry and Abdel-Rahman Ghoneim, "Optic Disc Detection from Normalized Digital Fundus Images by Means of a Vessels' Direction Matched Filter", *IEEE Transactions on Medical Imaging*, Vol. 27, No. 1, pp. 11 - 18, 2008.

[24] Mohammed Al-Rawi, Munib Qutaishat and Mohammed Arrar, "An improved matched Filter for blood vessel detection of digital retinal images", *Computers in Biology and Medicine*,Vol. 37, No. 2, pp. 262 – 267, 2007.

[25] Alireza Osareh, Majid Mirmehdi, Barry Thomas and Richard Markham, "Comparative Exudate Classification using Support Vector Machines and Neural Networks", *Medical Image Computing and Computer-Assisted Intervention*, *Lecture Notes in Computer Science*, Vol. 2489, pp. 413 – 420, 2002.

[26] Ahmad Fadzil M Hani, Hanung Adi Nugroho, Hermawan Nugroho, "Gaussian Bayes Classifier for Medical Diagnosis and Grading: Application to Diabetic Retinopathy", *IEEE EMBS Conference on Biomedical Engineering and Sciences*, pp. 52 – 56, 2010.

[27] http://en.wikipedia.org/wiki/Diabetes_mellitus

[28] http://www.advancedvisioncare.com/conditions.php

[29] http://en.wikipedia.org/wiki/Fundus_camera

[30] http://www.fink.com/papers/ee595/595.html

[31] T. Kauppi, V. Kalesnykiene, J. K. Kamarainen, L. Lensu, I. Sorri, H. Uusitalo, H. Kalviainen and J. Pietil, "DIARETDBO:Evaluation Database and Methodology for Diabetic Retinopathy Algorithms", Technical Report, Available: http://www.it.lut.fi/project/imageret/diaretdbO/2006, 2006.

[32] http://www.cs.um.edu.mt/~csaw/CSAW03/Proceedings/Support Vector Machines.pdf.

[33] http://www.statsoft.com/textbook/support-vector-machines/

[34] http://www.siue.edu/~sumbaug/RetinalProjectPapers/Diabetic%20Retinopathy%20Image%20Database%20Information.pdf.

[35] http://www.mathworks.in/help/toolbox/wavelet/ref/dwt2.html.

[36] http://home.dei.polimi.it/matteucc/Clustering/tutorial_html/cmeans.html.